

Europium(II) and Ytterbium(II) Cyclic Organohydroborates: An Europium(II) Complex with an Agostic Interaction

Xuenian Chen, Soyoung Lim, Christine E. Plečnik, Shengming Liu, Bin Du, Edward A. Meyers, and Sheldon G. Shore*

Department of Chemistry, The Ohio State University, Columbus, Ohio 43210

Received August 7, 2003

Lanthanide bis((cyclooctane-1,5-diyl)dihydroborate) complexes $(\text{THF})_4\text{Ln}\{(\mu\text{-H})_2\text{BC}_8\text{H}_{14}\}_2$ ($\text{Ln} = \text{Eu}$, **1**; Yb , **2**) were synthesized by a metathesis reaction between $(\text{THF})_x\text{LnCl}_2$ and $\text{K}[\text{H}_2\text{BC}_8\text{H}_{14}]$ in THF in a 1:2 molar ratio. Attempts to prepare the monosubstituted lanthanide cyclic organohydroborates $(\text{THF})_x\text{LnCl}\{(\mu\text{-H})_2\text{BC}_8\text{H}_{14}\}$ were unsuccessful. On the basis of the molecular structure and IR spectrum of **1**, there is an agostic interaction between Eu(II) and one of the $\alpha\text{-C-H}$ hydrogens from the $\{(\mu\text{-H})_2\text{BC}_8\text{H}_{14}\}$ unit. No such interaction was observed for **2**. The coordinated THF in **1** and **2** can be removed under dynamic vacuum, but the solvent ligands remain bound to Yb when **2** is directly dissolved in Et_2O or toluene. In strong Lewis basic solvents, such as pyridine or CH_3CN , attack of the Yb–H–B bridge bonds results. Decomposition of **2** to the 9-BBN dimer in CD_2Cl_2 was observed by ^{11}B and ^1H NMR spectroscopies. Compound **2** was reacted with 2 equiv of the hydride ion abstracting reagent $\text{B}(\text{C}_6\text{F}_5)_3$ to afford the solvent-separated ion pair $[\text{Yb}(\text{THF})_6][\text{HB}(\text{C}_6\text{F}_5)_3]_2$ (**3**). Complexes **1**, **2**, and **3** were characterized by single-crystal X-ray diffraction analysis. Crystal data: **1** is orthorhombic, $Pna2_1$, $a = 21.975(1)$ Å, $b = 9.310(1)$ Å, $c = 16.816(1)$ Å, $Z = 4$; **2** is triclinic, $P\bar{1}$, $a = 9.862(1)$ Å, $b = 10.227(1)$ Å, $c = 10.476(1)$ Å, $\alpha = 69.87(1)^\circ$, $\beta = 76.63(1)^\circ$, $\gamma = 66.12(1)^\circ$, $Z = 1$; **3**· Et_2O is triclinic, $P\bar{1}$, $a = 13.708(1)$ Å, $b = 14.946(1)$ Å, $c = 17.177(1)$ Å, $\alpha = 81.01(1)^\circ$, $\beta = 88.32(1)^\circ$, $\gamma = 88.54(1)^\circ$, $Z = 2$.

Introduction

Though all the lanthanides can exist in the divalent state in crystalline, alkaline earth metal halide lattices, only Sm(II), Eu(II), and Yb(II) are readily accessible under normal reaction conditions.^{1,2} The first divalent lanthanide metal-lacarborane complex, $[\text{Yb}(\text{C}_2\text{B}_9\text{H}_{11})(\text{DMF})_4]$, was reported by Hawthorne and co-workers.³ Shortly thereafter, our laboratory prepared a ytterbium(II) decaborate compound, $(\text{CH}_3\text{CN})_6\text{Yb}\{(\mu\text{-H})_2\text{B}_{10}\text{H}_{12}\} \cdot 2\text{CH}_3\text{CN}$, in which the $[\text{B}_{10}\text{H}_{14}]^{2-}$ unit coordinates to Yb(II) through two Yb–H–B bridge bonds.⁴ In addition to this work on polyhedral boron hydrides, abundant studies on Ln(III) tetrahydroborates have

been reported.⁵ However, there are few reports on divalent lanthanide $[\text{BH}_4]^-$ systems,⁶ and to the best of our knowledge, no synthetic studies have been published on lanthanide-(II) organohydroborates. It is worthy of note that Zanella et al.⁷ characterized the first actinide organohydroborate $\text{Cp}_3\text{U}\{(\mu\text{-H})_2\text{BC}_8\text{H}_{14}\}$ that incorporates the $[\text{H}_2\text{BC}_8\text{H}_{14}]^-$ ligand, the organohydroborate anion of the 9-BBN dimer.⁸

Recently, we synthesized a series of group 4 and 5 metallocene cyclic organohydroborate systems containing the $[\text{H}_2\text{BC}_4\text{H}_8]^-$, $[\text{H}_2\text{BC}_5\text{H}_{10}]^-$, and $[\text{H}_2\text{BC}_8\text{H}_{14}]^-$ ligands.⁹ Some of these complexes exhibit unusual reactivity with $\text{B}(\text{C}_6\text{F}_5)_3$ to afford cationic or neutral products according to the solvent's coordinating ability.^{10,11} In an effort to extend divalent lanthanide borohydride chemistry, the organohy-

* To whom correspondence should be addressed. E-mail: shore@chemistry.ohio-state.edu.

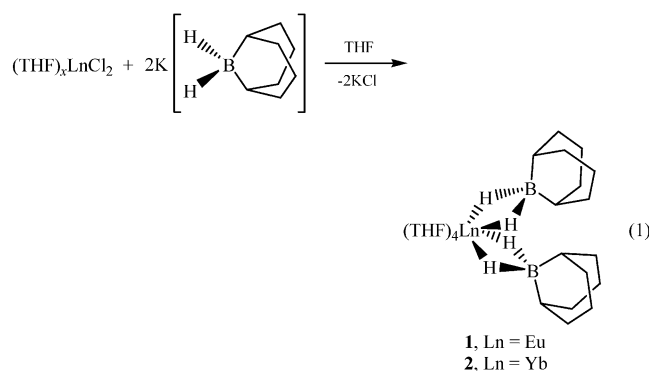
- (1) McClure, D. S.; Kiss, Z. *J. Chem. Phys.* **1963**, *39*, 3251.
- (2) Evans, W. J.; Allen, N. T.; Workman, P. S.; Meyer, J. C. *Inorg. Chem.* **2003**, *42*, 3097.
- (3) Manning, M. J.; Knobler, C. B.; Hawthorne, M. F. *J. Am. Chem. Soc.* **1988**, *110*, 4458.
- (4) (a) White, J. P., III; Deng, H.; Shore, S. G. *J. Am. Chem. Soc.* **1989**, *111*, 8946. (b) White, J. P., III; Shore, S. G. *Inorg. Chem.* **1992**, *31*, 2756.

- (5) (a) Marks, T. J.; Kolb, J. R. *Chem. Rev.* **1977**, *77*, 263. (b) Makhaev, V. D. *Russ. Chem. Rev.* **2000**, *69*, 727.
- (6) (a) White, J. P., III; Deng, H.; Shore, S. G. *Inorg. Chem.* **1991**, *30*, 2337. (b) Makhaev, V. D.; Borisov, A. P. *Z. Neorgan. Khim.* **1999**, *44*, 1489.
- (7) Zanella, P.; Ossola, F.; Porchia, M.; Rossetto, G.; Chiesi-Villa, A.; Guastini, C. *J. Organomet. Chem.* **1987**, *323*, 295.
- (8) (a) Köster, R.; Seidel, G. *Inorg. Chem.* **1983**, *22*, 198. (b) Brown, H. C.; Singaram, B.; Mathew, P. C. *J. Org. Chem.* **1981**, *46*, 2712.

droborate complexes $(\text{THF})_x\text{Ln}\{(\mu\text{-H})_2\text{BC}_8\text{H}_{14}\}_2$ ($\text{Ln} = \text{Eu}$, **1**; Yb , **2**) were prepared. A striking feature in the molecular structure of **1** is the existence of an agostic interaction between Eu(II) and the $\alpha\text{-C-H}$ bond of a $\{\text{H}_2\text{BC}_8\text{H}_{14}\}$ group. Although a number of agostic interactions involving Ln(III) have been reported,¹² examples of Ln(II) interactions are less abundant,¹³ and apparently, no Eu(II) cases appear to have been established previously. Here we provide details on the preparation, structural characterization, and reactivity of the lanthanide(II) disubstituted cyclic organohydroborates, **1** and **2**.

Results and Discussion

Preparation of $(\text{THF})_4\text{Ln}\{(\mu\text{-H})_2\text{BC}_8\text{H}_{14}\}_2$ ($\text{Ln} = \text{Eu}$, **1; Yb , **2**).** Lanthanide bis((cyclooctane-1,5-diy)l)dihydroborate complexes **1** and **2** are synthesized by reacting $(\text{THF})_x\text{LnCl}_2$ with $\text{K}[\text{H}_2\text{BC}_8\text{H}_{14}]$ in a 1:2 molar ratio at room temperature in THF (eq 1).

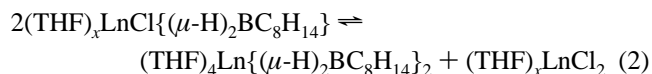


When the reagents are stirred overnight in Et_2O , no apparent reaction ensues since $(\text{THF})_x\text{LnCl}_2$ is insoluble in that solvent. Complexes **1** and **2** are stable in THF, Et_2O , and toluene solution. They are unstable in the solid state when they are stored at room temperature under vacuum or nitrogen. The solids lose the coordinating solvent, and their bright yellow color gradually changes to a faint yellow. The resulting materials are not soluble in Et_2O or toluene.

Attempts to prepare the monosubstituted lanthanide cyclic organohydroborates, $(\text{THF})_x\text{LnCl}\{(\mu\text{-H})_2\text{BC}_8\text{H}_{14}\}$, were unsuccessful. Slow dropwise addition of $\text{K}[\text{H}_2\text{BC}_8\text{H}_{14}]$ (1 equiv) in THF to a solution of $(\text{THF})_x\text{LnCl}_2$ afforded only the disubstituted complexes **1** and **2**. Boron-11 NMR spectra of the 1:1 reaction mixture of $(\text{THF})_x\text{YbCl}_2$ and $\text{K}[\text{H}_2\text{BC}_8\text{H}_{14}]$

revealed the presence of **2**. No other hydroborate complex was detected. Products from the 1:1 reactions were isolated and characterized by elemental analysis, single-crystal X-ray diffraction, ^1H NMR, and IR spectroscopy, all of which substantiated the formation of **1** and **2**.

The 1:1 complex $(\text{THF})_x\text{LnCl}\{(\mu\text{-H})_2\text{BC}_8\text{H}_{14}\}$ is probably formed as a transient intermediate, but a reverse metathesis reaction between two molecules of the monosubstituted derivative could occur, thereby producing $(\text{THF})_4\text{Ln}\{(\mu\text{-H})_2\text{BC}_8\text{H}_{14}\}_2$ and $(\text{THF})_x\text{LnCl}_2$. Since $(\text{THF})_x\text{LnCl}_2$ has limited solubility in THF, precipitation of the dichloride would drive the equilibrium on to the formation of the 1:2 complex (eq 2).



Molecular Structure of **1.** The molecular structure of **1** is shown in Figure 1. Crystal data are given in Table 1, and selected bond distances and angles are listed in Table 2. The coordination geometry about the Eu(II) center can be described as a distorted octahedron formed by two 9-BBN hydroborate ligands *cis* to each other and four THF ligands. Each 9-BBN hydroborate ligand is attached to Eu(II) through two Eu–H–B bridges. Of the $\text{Eu}\cdots\text{B}$ distances, 2.794(6) and 2.920(7) Å, the shorter distance is believed to be a consequence of an agostic interaction between Eu and the C(11)–H(11) bond that draws B(1) closer to Eu. The average Eu–O bond length is 2.61 Å. The B(1)–Eu–B(2) angle, 103.3(2)°, is considerably distorted from the regular *cis*-octahedral angle of 90°. The steric repulsion of the two

- (9) (a) Chen, X.; Liu, S.; Plečnik, C. E.; Liu, F.-C.; Fraenkel, G.; Shore, S. G. *Organometallics* **2003**, *22*, 275. (b) Liu, F.-C.; Plečnik, C. E.; Liu, S.; Liu, J.; Meyers, E. A.; Shore, S. G. *J. Organomet. Chem.* **2001**, *627*, 109. (c) Liu, F.-C.; Du, B.; Liu, J.; Meyers, E. A.; Shore, S. G. *Inorg. Chem.* **1999**, *38*, 3228. (d) Liu, F.-C.; Liu, J.; Meyers, E. A.; Shore, S. G. *Inorg. Chem.* **1998**, *37*, 3293. (e) Liu, J.; Meyers, E. A.; Shore, S. G. *Inorg. Chem.* **1998**, *37*, 496. (f) Jordan, G. T.; IV; Liu, F.-C.; Shore, S. G. *Inorg. Chem.* **1997**, *36*, 5597. (g) Jordan, G. T.; IV; Shore, S. G. *Inorg. Chem.* **1996**, *35*, 1087.
- (10) (a) Liu, S.; Liu, F.-C.; Renkes, G.; Shore, S. G. *Organometallics* **2001**, *20*, 5717. (b) Plečnik, C. E.; Liu, F.-C.; Liu, S.; Liu, J.; Meyers, E. A.; Shore, S. G. *Organometallics* **2001**, *20*, 3599. (c) Liu, F.-C.; Liu, J.; Meyers, E. A.; Shore, S. G. *J. Am. Chem. Soc.* **2000**, *122*, 6106.
- (11) (a) Yang, X.; Stern, C. L.; Marks, T. J.; Hartwig, J. F.; De Gala, S. R. *J. Am. Chem. Soc.* **1994**, *116*, 10015. (b) Antiñolo, A.; Carrillo-Hermosilla, F.; Fernández-Baeza, J.; García-Yuste, S.; Otero, A.; Sánchez-Prada, J.; Villaseñor, E. *J. Organomet. Chem.* **2000**, *609*, 123.

- (12) (a) Giesbrecht, G. R.; Gordon, J. C.; Brady, J. T.; Clark, D. L.; Keogh, D. W.; Michalczyk, R.; Scott, B. L.; Watkin, J. G. *Eur. J. Inorg. Chem.* **2002**, 723. (b) Klimpel, M. G.; Görlitzer, H. W.; Tafipolsky, M.; Spiegler, M.; Scherer, W.; Anwender, R. *J. Organomet. Chem.* **2002**, *647*, 236. (c) Qian, C.; Nie, W.; Sun, J. *Organometallics* **2000**, *19*, 4134. (d) Hieringer, W.; Eppinger, J.; Anwender, R.; Herrmann, W. *A. J. Am. Chem. Soc.* **2000**, *122*, 11983. (e) Klooster, W. T.; Brammer, L.; Schaverien, C. J.; Budzelaar, P. H. M. *J. Am. Chem. Soc.* **1999**, *121*, 1381. (f) Click, D. R.; Scott, B. L.; Watkin, J. G. *Chem. Commun.* **1999**, 633. (g) Evans, W. J.; Anwender, R.; Ziller, J. W.; Khan, S. I. *Inorg. Chem.* **1995**, *34*, 5927. (h) Procopio, L. L.; Carroll, P. J.; Berry, D. H. *J. Am. Chem. Soc.* **1994**, *116*, 177. (i) Barnhart, D. M.; Clark, D. L.; Gordon, J. C.; Huffman, J. C.; Watkin, J. G.; Zwick, B. D. *J. Am. Chem. Soc.* **1993**, *115*, 8461. (j) Schaverien, C. J.; Nesbitt, G. J. *J. Chem. Soc., Dalton Trans.* **1992**, 157. (k) Johns, V.; Koestlmeier, S.; Kotzian, M.; Roesch, N.; Watson, P. L. *Int. J. Quantum Chem.* **1992**, *44*, 853. (l) Reger, D. L.; Knox, S. J.; Lindeman, J. A.; Lieboda, L. *Inorg. Chem.* **1990**, *29*, 416. (m) Deacon, G. B.; Nickel, S.; MacKinnon, P.; Tiekink, E. R. T. *Aust. J. Chem.* **1990**, *43*, 1245. (n) Van der Heijden, H.; Schaverien, C. J.; Orpen, A. G. *Organometallics* **1989**, *8*, 255. (o) Heeres, H. J.; Meetsma, A.; Teuben, J. H.; Rogers, R. D. *Organometallics* **1989**, *8*, 2637. (p) Evans, W. J.; Chamberlain, L. R.; Ulibarri, T. A.; Ziller, J. W. *J. Am. Chem. Soc.* **1988**, *110*, 6423. (q) Heeres, H. J.; Meetsma, A.; Teuben, J. H. *J. Chem. Soc., Chem. Commun.* **1988**, 962. (r) Den Haan, K. H.; De Boer, J. L.; Teuben, J. H.; Spek, A. L.; Kojić-Prodić, B.; Hays, G. R.; Huis, R. *Organometallics* **1986**, *5*, 1726. (s) Jeske, G.; Schock, L. E.; Swepston, P. N.; Schumann, H.; Marks, T. L. *J. Am. Chem. Soc.* **1985**, *107*, 8103. (t) Tilley, T. D.; Andersen, R. A.; Zalkin, A. *J. Am. Chem. Soc.* **1982**, *104*, 3725.
- (13) (a) Nakamura, H.; Nakayama, Y.; Yasuda, H.; Maruo, T.; Kanehisa, N.; Kai, Y. *Organometallics* **2000**, *19*, 5392. (b) Rabe, G. W.; Riede, J.; Schier, A. *Organometallics* **1996**, *15*, 439. (c) Schwartz, D. J.; Ball, G. E.; Andersen, R. A. *J. Am. Chem. Soc.* **1995**, *117*, 6027. (d) Zhang, X.; McDonal, R.; Takats, J. *New J. Chem.* **1995**, *19*, 573. (e) Evans, W. J.; Hughes, L. A.; Hanusa, T. P. *J. Am. Chem. Soc.* **1984**, *106*, 4270.

Table 1. Crystallographic Data for (THF)₄Eu{(μ-H)₂BC₈H₁₄}₂ (**1**), (THF)₄{(μ-H)₂BC₈H₁₄}₂ (**2**), and [Yb(THF)₆][HB(C₆F₅)₃]₂ (**3**)

	1	2	3 ·Et ₂ O
empirical formula	C ₃₂ H ₆₄ B ₂ EuO ₄	C ₃₂ H ₆₄ B ₂ YbO ₄	C ₆₄ H ₆₁ B ₂ F ₃₀ YbO ₇ ^a
fw	686.41	707.58	1706.79
space group	<i>Pna</i> 2 ₁ (No. 33)	<i>P</i> 1̄ (No. 2)	<i>P</i> 1̄ (No. 2)
<i>a</i> , Å	21.975(1)	9.862(1)	13.708(1)
<i>b</i> , Å	9.310(1)	10.227(1)	14.946(1)
<i>c</i> , Å	16.816(1)	10.476(1)	17.177(1)
α, deg	90	69.87(1)	81.01(1)
β, deg	90	76.63(1)	88.32(1)
γ, deg	90	66.12(1)	88.54(1)
<i>V</i> , Å ³	3440.24(7)	901.8(2)	3473.5(4)
<i>Z</i>	4	1	2
<i>D</i> _{calcd} , g·cm ⁻³	1.325	1.295	1.632
<i>T</i> , °C	-123	-3	-73
<i>F</i> , mm ⁻¹	1.855	2.622	1.477
R1 [<i>I</i> > 2σ(<i>I</i>)] ^b	0.0314	0.0445	0.0478
wR2 (all data) ^c	0.0702	0.1101	0.1400

^a Substitutional disorder results in the following formula: [Yb(THF)_{5.5}(OEt₂)_{0.5}][HB(C₆F₅)₃]₂·Et₂O. ^b R1 = Σ||*F*_o| - |*F*_c||/Σ|*F*_o|. ^c wR2 = {Σw(*F*_o² - *F*_c²)/Σw(*F*_o²)^{1/2}.

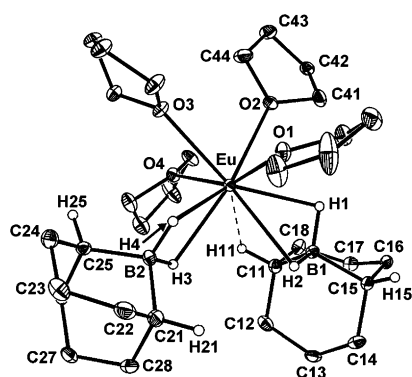


Figure 1. Molecular structure of (THF)₄Eu{(μ-H)₂BC₈H₁₄}₂ (**1**) showing 25% probability thermal ellipsoids. Bridging and α-C-H hydrogens are drawn with arbitrary thermal ellipsoids. All other hydrogen atoms are omitted for clarity.

Table 2. Selected Bond Distances and Angles for (THF)₄Eu{(μ-H)₂BC₈H₁₄}₂ (**1**)

Bond Distances (Å)			
Eu–O(1)	2.591(4)	Eu···B(2)	2.920(7)
Eu–O(2)	2.635(5)	B(1)–H(1)	1.17(4)
Eu–O(3)	2.597(3)	B(1)–H(2)	1.17(5)
Eu–O(4)	2.603(5)	B(2)–H(3)	1.25(5)
Eu–H(1)	2.48(4)	B(2)–H(4)	1.22(6)
Eu–H(2)	2.57(4)	Eu···C(15)	4.402
Eu–H(3)	2.43(6)	Eu···H(15)	4.800
Eu–H(4)	2.30(6)	Eu···C(21)	4.176
Eu–C(11)	3.116(6)	Eu···H(21)	4.190
Eu–H(11)	2.68(5)	Eu···C(25)	4.016
Eu···B(1)	2.794(6)	Eu···H(25)	3.956

Angles (deg)			
O(1)–Eu–O(2)	85.1(2)	B(1)–Eu–O(3)	171.5(2)
O(1)–Eu–O(3)	83.2(1)	B(1)–Eu–O(4)	109.5(2)
O(1)–Eu–O(4)	155.9(2)	Eu–B(1)–C(11)	85.5(3)
O(2)–Eu–O(3)	77.9(1)	Eu–B(1)–C(15)	168.2(4)
O(2)–Eu–O(4)	79.2(1)	Eu–B(2)–C(21)	131.2(4)
O(3)–Eu–O(4)	75.8(1)	Eu–B(2)–C(25)	122.7(5)
B(1)–Eu–B(2)	103.3(2)	B(1)–C(11)–H(11)	119(3)
B(1)–Eu–O(1)	90.2(2)	B(1)–C(15)–H(15)	115(3)
B(1)–Eu–O(2)	96.2(2)		

{(μ-H)₂BC₈H₁₄} units forces the THF ligands toward each other; the O(1)–Eu–O(4) angle between *trans*-THF ligands is 155.9(2)° and one of the *cis*-THF angles, O(2)–Eu–O(3), measures 77.9(1)°.

A comparison of the interactions between Eu and the two cyclic organohydroborate ligands reveals a significant struc-

tural difference. In the {(μ-H)₂BC₈H₁₄} ligand that contains B(1), the Eu–C(11) distance of 3.116(6) Å is more than 1 Å shorter than the distance of Eu to the other α-carbon (C(15); 4.402 Å). Additionally, the Eu–B(1)–C(11) angle of 85.5(3)° is much smaller than the corresponding Eu–B(1)–C(15) angle of 168.2(4)°. Such distortion results from an agostic interaction between the C(11)–H(11) bond and the Eu atom. The Eu–H(11) distance 2.68(5) Å, is within 3 esd's of the Eu–H–B(1) bridge bonds (Eu–H(1), 2.48(4) Å; Eu–H(2), 2.57(4) Å). That this is an agostic interaction is further supported by the presence of a band at 2760 cm⁻¹ in the IR spectrum of **1**. The distance of Eu to the other α-hydrogen, H(15), is 4.800 Å well beyond consideration for an *agostic* interaction.

On the other hand, the {(μ-H)₂BC₈H₁₄} moiety involving B(2) coordinates symmetrically to Eu. This symmetric coordination constrains the distances, Eu···C(21) (4.176 Å) and Eu···C(25) (4.016 Å), and angles, Eu–B(2)–C(21) (131.2(4)°) and Eu–B(2)–C(25) (122.7(5)°), to be similar. The distance of Eu to the α-hydrogens, H(21) and H(25) (average 4.073 Å), is well outside the range anticipated for an agostic interaction.¹⁴ The two Eu–H–B(2) bridge bonds (Eu–H(3), 2.43(6) Å; Eu–H(4), 2.30(6) Å) appear to be shorter than those for Eu–H–B(1).

Molecular Structure of 2. The molecular structure of **2** is shown in Figure 2. Crystal data and selected bond distances and angles are provided in Tables 1 and 3. The asymmetric unit is comprised of Yb(1) on an inversion center, one {(μ-H)₂BC₈H₁₄} unit, and two THF solvent ligands. Inversion through the Yb(II) center generates the remainder of the molecule. The THF ligands are disordered, with each ligand adopting two positions with ca. 50% occupancy. Only one of these arrangements is shown in Figure 2. The full set of THF orientations is depicted in the Supporting Information.

The coordination geometry around the Yb(II) atom consists of a distorted octahedral arrangement of two {(μ-H)₂BC₈H₁₄} groups and four THF ligands. The {(μ-H)₂BC₈H₁₄} units are

(14) (a) Brookhart, M.; Green, M. L. H.; Wong, L.-L. *Prog. Inorg. Chem.* **1988**, *36*, 1. (b) Crabtree, R. H.; Hamilton, D. G. *Adv. Organomet. Chem.* **1988**, *28*, 299. (c) Brookhart, M.; Green, M. L. H. *J. Organomet. Chem.* **1983**, *250*, 395.

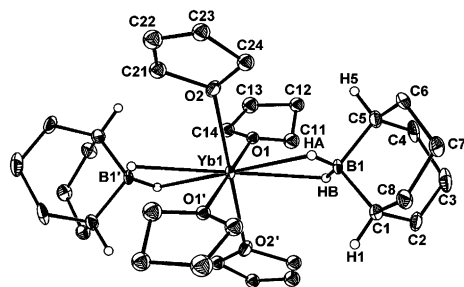


Figure 2. Molecular structure of $(\text{THF})_4\text{Yb}\{(\mu\text{-H})_2\text{BC}_8\text{H}_{14}\}_2$ (**2**) showing 15% probability thermal ellipsoids. Bridging and $\alpha\text{-C-H}$ hydrogens are drawn with arbitrary thermal ellipsoids. All other hydrogen atoms are omitted for clarity.

Table 3. Selected Bond Distances and Angles for $(\text{THF})_4\text{Yb}\{(\mu\text{-H})_2\text{BC}_8\text{H}_{14}\}_2$ (**2**)^a

Bond Distances (Å)			
Yb(1)···B(1)	2.876(7)	B(1)–H(A)	1.09(11)
Yb(1)–H(A)	2.59(11)	B(1)–H(B)	1.15(12)
Yb(1)–H(B)	2.59(13)	B(1)–C(1)	1.59(1)
Yb(1)–O(1)	2.424(11)	B(1)–C(5)	1.59(1)
Yb(1)–O(2)	2.462(6)		
Angles (deg)			
H(A)–Yb(1)–H(B)	46(3)	O(1)–Yb(1)–H(A)	104(2)
H(A)–B(1)–H(B)	128(9)	O(1)–Yb(1)–H(B)	70(3)
O(1)–Yb(1)–O(2)	94.7(4)	O(2)–Yb(1)–H(A)	74(2)
O(1)–Yb(1)–B(1)	87.7(3)	O(2)–Yb(1)–H(B)	106(3)
O(2)–Yb(1)–B(1)	89.9(2)		

^a Symmetry transformation used to generate equivalent atoms: $-x + 2, -y - 2, -z$.

trans to each other along the elongated axis, and each is bound to Yb though two Yb–H–B bridges. Equatorial oxygen atoms of the THF ligands are coplanar with Yb(II). The THF rings are parallel to each other and are perpendicular to the equatorial plane. This differs from the $\text{C}_5\text{H}_5\text{N}$ ring arrangement, “four-bladed right- and left-handed propellers,” in $(\text{C}_5\text{H}_5\text{N})_4\text{Yb}(\text{BH}_4)_2$.^{6a}

The Yb–O distances, 2.421(11) and 2.462(6) Å, compare favorably with those in $\text{Cp}_2\text{Yb}(\text{THF})$ (2.412(5) Å)¹⁵ and $\eta^5\text{-bis}(\text{Pr-indenyl})\text{Yb}(\text{THF})_2$ (2.47(1), 2.77(7) Å).^{13a} The Yb(1)–H(A) and Yb(1)–H(B) distances of the Yb(1)–H–B bridges are 2.59(11) Å and 2.59(13) Å. The Yb···B distance of 2.876(7) Å is noticeably longer than the 2.666(6) and 2.692(5) Å lengths in $(\text{CH}_3\text{CN})_4\text{Yb}(\text{BH}_4)_2$ and $(\text{C}_5\text{H}_5\text{N})_4\text{Yb}(\text{BH}_4)_2$.^{6a} This dissimilarity mainly results from the two distinct coordination modes of the ligands; $[\text{H}_2\text{BC}_8\text{H}_{14}]^-$ is bidentate while $[\text{BH}_4]^-$ is tridentate.^{6a} Variations in M···B distances between complexes with μ_2 - and μ_3 - BH_4 coordination modes typically fall within the range 0.16–0.34 Å.^{5b} In contrast, compounds having bidentate borohydride ligands, such as $[\text{H}_2\text{BC}_8\text{H}_{14}]^-$, $[\text{H}_2\text{BC}_4\text{H}_8]^-$, $[\text{H}_2\text{BC}_5\text{H}_{10}]^-$, and $[\text{H}_2\text{BH}_2]^-$, do not differ significantly in their M···B distances.⁹ Besides affecting the Yb···B distance, the coordination mode also influences the stability of the organohydroborate and borohydride complexes. For instance, the doubly bridged system in **2** is prone to attack by strong Lewis basic solvents, whereas triply bridged lanthanide tetrahydroborates are stable in those solvents.^{6a}

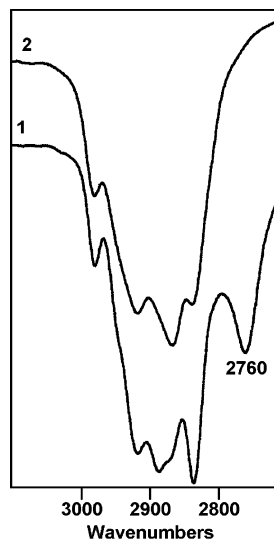


Figure 3. Solid-state (KBr) IR spectra of the complexes $(\text{THF})_4\text{Eu}\{(\mu\text{-H})_2\text{BC}_8\text{H}_{14}\}_2$ (**1**) and $(\text{THF})_4\text{Yb}\{(\mu\text{-H})_2\text{BC}_8\text{H}_{14}\}_2$ (**2**) in the C–H stretching region.

Comments on the Differences between the Structures of **1 and **2**.** As reported above the solid-state structure of complex **1** possesses a *cis* arrangement of $[\text{H}_2\text{BC}_8\text{H}_{14}]^-$ ligands while a *trans* arrangement occurs in complex **2**. Analysis of crystal packing gives no obvious reasons for the difference between these two structures. On steric grounds the *trans* arrangement is favored. Thus, the occurrence of the *cis* arrangement most likely implies the influence of the *agostic* bond. The question arises as to why the two complexes are structurally different. As indicated from IR spectra, below the *agostic* interaction occurs in solution as well as in the solid state. In the simplest terms, on the basis of charge density, size of the metal with respect to radius, ytterbium would be expected to be more likely to interact with the $\alpha\text{-C-H}$ hydrogen because of its higher positive charge density. However, the larger size of the europium favors a larger coordination number and this might be the driving factor for the formation of the *agostic* bond.

IR and NMR Spectra. Complexes **1** and **2** generally exhibit similar IR spectra in the solid-state. Bands assigned to Ln–H–B stretches appear from 2012 to 2075 cm^{-1} for **1** and from 2035 to 2118 cm^{-1} for **2**. A striking discrepancy between the spectra is apparent in the C–H stretching region. Besides the normal C–H stretches from 2979 to 2834 cm^{-1} , an additional absorption at a lower frequency, 2760 cm^{-1} , is present in **1**'s spectrum (Figure 3). The appearance of this extra stretch is consistent with an *agostic* interaction between Eu(II) and an $\alpha\text{-C-H}$ bond of the organohydroborate ring.^{12a,i} An IR spectrum of **1** in benzene solution displays a weak broad shoulder at 2759 cm^{-1} . Not unexpectedly, the *agostic* interaction is weaker in solution than in the solid state. It is of interest to note that IR evidence for *agostic* interactions between a C–H bond and a lanthanide metal are relatively rare^{12a,f,g} compared to such interactions between a C–H bond and a transition metal,¹⁶ the first example of which was suggested by Trofimenko^{16d} based upon IR and ¹H NMR spectra and later established by Cotton and co-workers¹⁷ through single-crystal X-ray analysis.

(15) Tilley, T. D.; Andersen, R. A.; Spencer, B.; Ruben, H.; Zalkin, A.; Templeton, D. H. *Inorg. Chem.* **1980**, *19*, 2999.

The paramagnetism of the Eu(II) atom (f^7) in **1** prevents the acquisition of NMR spectra that are easily interpreted. However, Yb(II) (f^{14}) is diamagnetic, and NMR spectra for **2** were acquired in a variety of solvents (see Experimental Section).

The ^{11}B NMR spectrum of **2** in THF consists of a triplet at $\delta -11.2$ ($^1J_{\text{BH}} = 69$ Hz), which is downfield relative to the signal of the precursor $\text{K}[\text{H}_2\text{BC}_8\text{H}_{14}]$ ($\delta -16.3$; $^1J_{\text{BH}} = 73$ Hz).^{8b} Triplets are also apparent in the ^{11}B NMR spectra of **2** in Et_2O ($\delta -9.5$; $^1J_{\text{BH}} = 65$ Hz) and toluene ($\delta -10.1$; $^1J_{\text{BH}} = 65$ Hz).

The ^1H NMR spectrum of **2** in d_8 -THF includes a broad multiplet from $\delta 1.84$ to 1.41 and a singlet at $\delta 0.84$. The former is designated as the β - and γ -hydrogens of the organohydroborate ring and the latter is assigned to the α -protons.^{9a} The bridging hydrogen resonance, $\delta 1.63$, was located by comparing the ^1H and $^1\text{H}\{^{11}\text{B}\}$ NMR spectra. Proton spectra of **2** in d_{10} - Et_2O and d_8 -toluene have similar chemical shifts for the $\{(\mu\text{-H})_2\text{BC}_8\text{H}_{14}\}$ unit, but peaks corresponding to the α -hydrogens of ligated THF (d_{10} - Et_2O , $\delta 3.92$; d_8 -Tol, $\delta 4.06$) are also visible. The signal from the β -hydrogens of the THF ring overlaps with the multiplet for the organohydroborate β - and γ -protons.

The procedure of stirring **2** in Et_2O , removing the solvent, and redissolving the solid in Et_2O promotes the complete replacement of THF by Et_2O and forms $(\text{Et}_2\text{O})_x\text{Yb}\{(\mu\text{-H})_2\text{BC}_8\text{H}_{14}\}_2$. The ^1H NMR spectrum of this solid dissolved in ether does not contain any THF resonances. In turn, the solid can be redissolved in d_8 -THF, and the ^1H NMR spectrum illustrates that the coordinated Et_2O molecules in $(\text{Et}_2\text{O})_x\text{Yb}\{(\mu\text{-H})_2\text{BC}_8\text{H}_{14}\}_2$ are displaced by the stronger nucleophile THF to regenerate **2**.

Reactions occur when **2** is dissolved in the strong Lewis basic solvents pyridine and CH_3CN . Symmetrical cleavage of the double hydrogen bridge transpires in pyridine to generate the $\text{HBC}_8\text{H}_{14}\cdot\text{Pyr}$ adduct. In the ^{11}B NMR spectrum of **2** in pyridine, two signals, a broad unresolved doublet at $\delta -1.6$ for $\text{HBC}_8\text{H}_{14}\cdot\text{Pyr}$ and a triplet at $\delta -9.6$ for **2**, are evident. (The chemical shift of the $\text{HBC}_8\text{H}_{14}\cdot\text{Pyr}$ adduct was verified by acquiring the ^{11}B NMR spectrum of the 9-BBN dimer in pyridine.) Since the intensity ratio of the two peaks did not alter over time, the system may exist in equilibrium. Besides $\text{HBC}_8\text{H}_{14}\cdot\text{Pyr}$, we were unable to identify the other cleavage product. The reaction between **2** and CH_3CN is less obvious. After 30 min, the ^{11}B NMR spectrum of **2** in CH_3CN contains the signal for **2** ($\delta -10.3$) and a downfield singlet at $\delta 48.5$ for a trialkyl borane. After 1 day, the intensity of the organoborane peak gradually increases, while **2**'s resonance disappears.

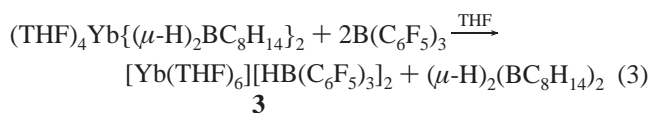
Table 4. Selected Bond Distances and Angles for $[\text{Yb}(\text{THF})_{5.5}(\text{Et}_2\text{O})_{0.5}][\text{HB}(\text{C}_6\text{F}_5)_3]_2$ (**3**)^a

Bond Distances (Å)			
Yb(1)–O(1)	2.376(4)	Yb(2)–O(5)	2.387(4)
Yb(1)–O(2)	2.384(3)	Yb(2)–O(6)	2.411(4)
Yb(1)–O(3)	2.389(4)	B(1)–H(1)	1.09(5)
Yb(2)–O(4)	2.399(4)	B(2)–H(2)	1.10(5)
Angles (deg)			
O(1)–Yb(1)–O(2)	90.0(1)	O(4)–Yb(2)–O(5)	91.0(2)
O(1)–Yb(1)–O(3)	90.7(2)	O(4)–Yb(2)–O(6)	87.3(2)
O(2)–Yb(1)–O(3)	90.8(1)	O(5)–Yb(2)–O(6)	88.6(1)

^a Symmetry transformations used to generate equivalent atoms: (A) $-x, -y + 1, -z$; (B) $-x + 1, -y, -z + 1$.

Dissolution of **2** in CH_2Cl_2 produces a white precipitate in a colorless solution. The ^{11}B NMR spectrum consists of one signal at $\delta 27.2$, which is assigned to the 9-BBN dimer.^{9a} The ^1H NMR spectrum of **2** in CD_2Cl_2 confirms the formation of the 9-BBN dimer.^{9a} Though clearly the $\{\text{HBC}_8\text{H}_{14}\}$ moieties in **2** dimerize, the resulting environment around the Yb(II) center is uncertain.

Reactions with $\text{B}(\text{C}_6\text{F}_5)_3$. Treatment of **2** with 2 equiv of the hydride ion abstracting reagent $\text{B}(\text{C}_6\text{F}_5)_3$ yields the solvent-separated ion pair complex $[\text{Yb}(\text{THF})_6][\text{HB}(\text{C}_6\text{F}_5)_3]_2$ (**3**) and the 9-BBN dimer, $(\mu\text{-H})_2(\text{BC}_8\text{H}_{14})_2$ (eq 3). On the basis of an ^{11}B NMR spectrum of the reaction solution, the



anion $[\text{HB}(\text{C}_6\text{F}_5)_3]^-$ and the 9-BBN dimer (28.7 ppm) were formed in less than 30 min. With increasing time, the 9-BBN dimer changed to the trialkyl borane ($\delta 57.6$), which is also produced in the abstraction reaction between $\text{Cp}_2\text{Ti}\{(\mu\text{-H})_2\text{BC}_8\text{H}_{14}\}$ and $\text{B}(\text{C}_6\text{F}_5)_3$.^{10b} The ^{11}B NMR spectrum of **3** in THF consists of a doublet ($^1J_{\text{BH}} = 90$ Hz) at $\delta -24.5$, which is consistent with the $[\text{HB}(\text{C}_6\text{F}_5)_3]^-$ anion.

Crystals of **3** were grown from a saturated Et_2O solution and contained 2 mol of Et_2O per unit cell as solvent of crystallization. The cations are on inversion centers. There are two unique $[\text{HB}(\text{C}_6\text{F}_5)_3]^-$ anions in the asymmetric unit. The boron atoms have approximate tetrahedral geometry and their structural features are not unusual,¹⁰ although some disorder is observed in the C_6F_5 groups of one of the anions. There are two unique cations in the unit cell, each of which having Yb^{2+} surrounded by six oxygen atoms in an approximately octahedral configuration (average Yb–O, 2.39 Å; parameter O–Yb–O, 89.7°; Table 4). These structural parameters closely resemble those of the similar cation in $[\text{Yb}(\text{THF})_6][\text{Co}(\text{CO})_4]_2$ (average Yb–O, 2.388 Å; average O–Yb–O, 90.0°).¹⁸ Both cations in this structure are disordered. One of these, $\text{Yb1}(\text{THF})_6^{2+}$, is shown in Figure 4 with the positionally disordered atoms C22', C32', and C33' omitted for clarity. The second cation, $[\text{Yb}_2(\text{THF})_6]^{2+}$, in addition to positional disorder in the equatorial THF ligands, has both THF and Et_2O present in the axial positions, each

- (16) (a) McGrady, G. S.; Downs, A. J.; Haaland, A.; Scherer, W.; McKean, D. C. *Chem. Commun.* **1997**, 1547. (b) Jordan, R. F.; Bradley, P. K.; Baenziger, N.; LaPointe, R. E. *J. Am. Chem. Soc.* **1990**, *112*, 1289. (c) Thompson, M. E.; Baxter, S. M.; Bulls, A. R.; Burger, B. J.; Nolan, M. C.; Santarsiero, B. D.; Schaefer, W. P.; Bercaw, J. E. *J. Am. Chem. Soc.* **1987**, *109*, 203. (d) Trofimenko, S. *Inorg. Chem.* **1970**, *11*, 2493. (e) Trofimenko, S. *J. Am. Chem. Soc.* **1968**, *90*, 4754.
- (17) (a) Cotton, F. A.; Frenz, B. A.; Stanislawski, A. G. *Inorg. Chim. Acta* **1973**, *7*, 503. (b) Cotton, F. A.; Jeremic, M.; Shaver, A. *Inorg. Chim. Acta* **1972**, *6*, 543.

- (18) Plečnik, C. E.; Liu, S.; Liu, J.; Chen, X.; Meyers, E. A.; Shore, S. G. *Inorg. Chem.* **2002**, *41*, 4936.

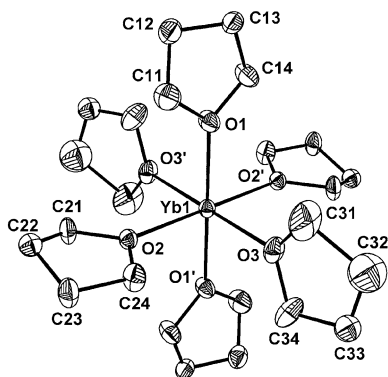


Figure 4. Molecular structure of the cation in $[\text{Yb}(\text{THF})_6][\text{HB}(\text{C}_6\text{F}_5)_3]_2$ (**3**) showing 25% probability thermal ellipsoids. Hydrogen atoms are omitted for clarity.

with approximately 50% occupancy. Detailed representations of the anions and cations are given in the Supporting Information.

Experimental Section

General Comments. All manipulations were carried out on a standard high vacuum line or in a drybox under an atmosphere of nitrogen. Tetrahydrofuran, diethyl ether, toluene, and pyridine were dried over sodium/benzophenone and freshly distilled prior to use. Acetonitrile and methylene chloride were stirred over P_2O_5 for 10 days before being distilled for use. Hexane was stirred over concentrated sulfuric acid for 2 days and then decanted and washed with water. Next the hexane was stirred over sodium/benzophenone for 1 week, followed by distillation into a storage bulb containing sodium/benzophenone. Celite was dried by heating at 150°C under dynamic vacuum for 5 h. Ammonia (Matheson) was distilled from sodium immediately prior to use. Ammonium chloride (Fisher) was recrystallized from anhydrous methanol and vacuum-dried at 120°C prior to use. Ytterbium metal (40 mesh, Strem) was used as received. Europium (ingot, Strem) was packaged under mineral oil, washed with hexane, and vacuum-dried. The metal was cut into small pieces before use. Tetrahydrofuran-free $\text{K}[\text{H}_2\text{BC}_8\text{H}_{14}]$ was prepared according to the literature procedure.^{8a} Potassium hydride (Aldrich) was received as an oil slurry, washed with hexane, vacuum-dried, and stored in the drybox. 9-Borabicyclo[3.3.1]nonane dimer (Aldrich) was used as received. Solvated lanthanide dichlorides were synthesized according to the published method¹⁹ with the modifications listed below. Elemental analyses were performed by Galbraith Laboratories, Inc., Knoxville, TN. NMR spectra were recorded on a Bruker AM-250 spectrometer. ^1H NMR spectra were obtained at 250.1 MHz, and referenced to residual solvent protons. ^{11}B NMR spectra were obtained at 80.3 MHz, and externally referenced to $\text{BF}_3\cdot\text{OEt}_2$ in C_6D_6 ($\delta = 0.00$ ppm). Infrared spectra were recorded on a Mattson-Polaris FT-IR spectrometer with 2 cm^{-1} resolution.

X-ray Structure Determination. Single-crystal X-ray diffraction data were collected on a Nonius KappaCCD diffraction system, which employs graphite-monochromated $\text{Mo}-\text{K}\alpha$ radiation ($\lambda = 0.71073$). Single crystals of **1**, **2**, and **3** were each mounted on the tip of a glass fiber coated with Fomblin oil (a pentafluoropolyether). Unit cell parameters were obtained by indexing the peaks in the first 10 frames and refined by employing the whole data set. All frames were integrated and corrected for Lorentz and polarization effects using the DENZO-SMN package (Nonius BV, 1999).²⁰

The empirical absorption correction was applied with the SORTAV program²¹ provided by MaXus software.²² The positions of the heavy atoms, Yb and Eu, were revealed by the Patterson method. The structures were refined using the SHELXTL-97 (difference electron density calculations and full-matrix least-squares refinements) structure solution package.²³ Data merging was performed using the data preparation program supplied by SHELXTL-97. After all non-hydrogen atoms were located and refined anisotropically, hydrogen atom positions were calculated assuming standard geometries. Bridge hydrogens in **1** and **2**, the α -hydrogens of the organohydroborate ring in **1**, and the terminal B–H hydrogens of the anions in **3** were located and refined isotropically.

The Yb atom in **2** resides on a special position, $(1, -1, 0)$. Tetrahydrofuran ligands in **2** are disordered; two random orientations were resolved for each ligand. The atoms were split and the occupancies were refined isotropically. Positions of the hydrogen atoms on the disordered THF carbons were not calculated. The two Yb atoms in **3** are located on special positions (Yb(1), $(0, 1/2, 0)$; Yb(2), $(1/2, 0, 1/2)$). Some of the THF carbon atoms and pentafluorophenyl carbon and fluorine atoms are disordered. Additionally, substitutional disorder is observed in the cation with Yb(2); carbon atoms bonded to O(4) are distributed over two sites, THF or Et_2O carbon positions, and each component contributes approximately 50%. Thus, the formula is $[\text{Yb}(\text{THF})_{5.5}(\text{OEt}_2)_{0.5}][\text{HB}(\text{C}_6\text{F}_5)_3]_2\cdot\text{Et}_2\text{O}$ which includes a molecule of cocrystallized Et_2O . The disorder in **3** was treated in the same manner as it was for **2**.

Preparation of $(\text{THF})_4\text{Eu}\{(\mu\text{-H})_2\text{BC}_8\text{H}_{14}\}_2$, **1.** In a drybox, a 50 mL flask containing a Teflon-coated magnetic stir bar was charged with 152 mg (1.00 mmol) of Eu metal and 107 mg (2.00 mmol) of NH_4Cl . The flask was connected to a vacuum line and evacuated. Ammonia (25 mL, liquid) was condensed into the flask at -78°C and stirred at that temperature. A reaction occurred immediately with evolution of H_2 and formation of a golden-yellow suspension. After 40 min of stirring, the NH_3 was removed in vacuo and a light gray-colored solid, $(\text{NH}_3)_x\text{EuCl}_2$, remained. $(\text{THF})_x\text{EuCl}_2$ was prepared by stirring the NH_3 -solvated complex in THF, pumping off the solvent, and repeating this procedure two more times to ensure that all of the ammonia was replaced. The flask was then charged with 324 mg (2.00 mmol) of $\text{K}[\text{H}_2\text{BC}_8\text{H}_{14}]$ in the drybox and evacuated. Next, 25 mL of THF was condensed into the flask at -78°C , and the mixture was warmed to room temperature and stirred overnight. During this time the color of the solution changed to an orange-brown with formation of a precipitate. Filtration of the reaction mixture yielded a yellow-brown colored filtrate. The filtrate was cooled to 0°C and slow removal of the THF solvent under vacuum provided yellow X-ray quality crystals of **1**. Complete removal of the solvent at room temperature gave a yellow solid, which became faint yellow after washing with hexane and vacuum-drying. As determined by elemental analysis, this procedure promoted the loss of three THF ligands ($(\text{THF})_x\text{Eu}\{(\mu\text{-H})_2\text{BC}_8\text{H}_{14}\}_2$). Anal. Calcd for $\text{C}_{20}\text{H}_{40}\text{O}_2\text{EuB}_2$ (loss of three THF solvent ligands): C, 51.08; H, 8.57; B, 4.60. Found: C, 50.81; H,

(20) Otwinowsky, Z.; Minor, W. Processing of X-ray Diffraction Data Collected in Oscillation Mode. In *Macromolecular Crystallography, Part A*; Carter, C. W., Jr., Sweet, R. M., Eds.; Methods in Enzymology 276; Academic Press: New York, 1997; pp 307–326.

(21) (a) Blessing, R. H. *Acta Crystallogr.* **1995**, *51A*, 33. (b) Blessing, R. H. *J. Appl. Crystallogr.* **1997**, *30*, 421.

(22) Mackay, S.; Gilmore, C. J.; Edwards, C.; Tremayne, M.; Stuart, N.; Shankland, K. *MaXus: A Computer Program for the Solution and Refinement of Crystal Structures from Diffraction Data*; University of Glasgow: Glasgow, Scotland, Nonius BV: Delft, The Netherlands, and MacScience Co. Ltd.: Yokohama, Japan, 1998.

(23) Sheldrick, G. M. *SHELXTL-97: A Structure Solution and Refinement Program*; University of Göttingen: Germany, 1998.

(19) Howell, J. K.; Pytlewski, L. L. *J. Less Common Met.* **1969**, *18*, 437.

8.20; B, 4.58. A yield of 406 mg of (THF)Eu{(μ -H)₂BC₈H₁₄}₂ (86% based on K[H₂BC₈H₁₄]) was obtained. Solid-state IR (KBr): 2979 (s), 2918 (vs), 2887 (vs), 2837 (vs), 2760 (s), 2688 (w), 2657 (w), 2075 (s), 2012 (m), 1651 (w), 1557 (w), 1539 (m), 1446 (m), 1402 (m), 1336 (w), 1313 (w), 1282 (w), 1232 (m), 1103 (w), 1079 (w), 1038 (m), 988 (w), 952 (w), 927 (w), 891 (w), 819 (m), 744 (w) cm⁻¹. Solution IR (benzene, ν_{C-H}): 2976 (s), 2917 (vs), 2892 (s), 2869 (vs), 2837 (vs), 2759 (br, sh) cm⁻¹.

Preparation of (THF)₄Yb{(μ -H)₂BC₈H₁₄}₂, **2.** In a procedure similar to the one described above for **1**, 173 mg (1.00 mmol) of Yb metal and 107 mg (2.00 mmol) of NH₄Cl were reacted in 25 mL of NH₃. The light green solid (NH₃)_xYbCl₂ was converted to (THF)_xYbCl₂, which was combined with 324 mg (2.00 mmol) of K[H₂BC₈H₁₄] in 25 mL of THF. The mixture was stirred overnight, during which time the color of the solution changed to orange-brown with formation of a precipitate. Filtration of the reaction mixture yielded a yellow-brown colored filtrate. The filtrate was cooled to 0 °C and slow removal of the solvent afforded yellow X-ray quality crystals of **2**. Complete removal of the solvent at room temperature gave a yellow solid, which became faint yellow after being washed with hexane and vacuum-dried. As determined by elemental analysis, this procedure promoted the loss of two THF ligands ((THF)₂Yb{(μ -H)₂BC₈H₁₄}). Anal. Calcd for C₂₄H₄₈O₂-YbB₂ (loss of two THF solvent ligands): C, 51.17; H, 8.59; B, 3.84. Found: C, 50.97; H, 8.48; B, 3.74. A yield of 497 mg of (THF)₂Yb{(μ -H)₂BC₈H₁₄}₂ (88% based on K[H₂BC₈H₁₄]) was obtained. Solid-state IR (KBr): 2975 (s), 2913 (vs), 2863 (vs), 2834 (vs), 2684 (w), 2655 (w), 2118 (m), 2087 (m), 2035 (m), 1696 (m), 1649 (m), 1556 (m), 1450 (m), 1413 (m), 1335 (m), 1283 (m), 1205 (m), 1158 (w), 1105 (w), 1037 (s), 881 (w), 822 (w), 798 (w) cm⁻¹. ¹¹B NMR (80 MHz, THF): δ -11.2 (t, ¹J_{BH} = 69 Hz). ¹H NMR (250 MHz, *d*₈-THF): δ 1.84–1.41 (m, β - and γ -H of {(μ -H)₂BC₈H₁₄}, β -H of THF), 0.84 (s, α -H of {(μ -H)₂BC₈H₁₄}). ¹H{¹¹B} NMR (250 MHz, *d*₈-THF): δ 1.63 (s, μ -H). ¹¹B NMR (80 MHz, Tol): δ -10.1 (t, ¹J_{BH} = 65 Hz). ¹H NMR (250 MHz, *d*₈-Tol): δ 4.06 (br s, α -H of THF), 2.23–1.46 (m, β - and γ -H of {(μ -H)₂BC₈H₁₄}, β -H of THF), 1.23 (s, α -H of {(μ -H)₂BC₈H₁₄}). ¹H{¹¹B} NMR (250 MHz, *d*₈-Tol): δ 1.82 (s, μ -H). ¹¹B NMR (80 MHz, Et₂O): δ -9.5 (t, ¹J_{BH} = 65 Hz). ¹H NMR (250 MHz, *d*₁₀-Et₂O): δ 3.92 (br s, α -H of THF), 1.90–1.50 (m, β - and γ -H of {(μ -H)₂BC₈H₁₄}, β -H of THF), 0.89 (s, α -H of {(μ -H)₂BC₈H₁₄}). ¹H{¹¹B} NMR (250 MHz, *d*₁₀-Et₂O): δ 1.68 (s, μ -H).

Reaction of **2 with Pyridine, CH₃CN, and CD₂Cl₂. A. Pyridine.** Complex **2** (12 mg, 0.02 mmol) was dissolved in 0.5 mL of pyridine in a NMR tube. The color of the solution was violet. The tube was attached to the vacuum line, cooled to -78 °C, evacuated, and flame-sealed. The ¹¹B NMR spectrum (80 MHz) of the reaction solution included two resonances, δ -1.6 for HBC₈H₁₄·Pyr and δ -9.6 for **2**. The ratio (approximately 1:3) of the two peaks did not change with time. The chemical shift of the 9-BBN adduct was verified by dissolving the 9-BBN dimer in pyridine.

B. CH₃CN. In a NMR tube, **2** was dissolved in CH₃CN, and the color of the solution changed from yellow to orange. After 30 min

at room temperature, the ¹¹B NMR spectrum (80 MHz) of the reaction solution contained two signals, δ 48.5 for an organoborane and δ -10.3 for **2**. The ratio of organoborane to **2** was 0.04. This ratio changed over time: 2 h, 0.14; 5 h, 0.30; 10 h, 1.20. After 24 h, **2** completely reacted with CH₃CN to form the organoborane.

C. CD₂Cl₂. When **2** was dissolved in CD₂Cl₂ in a NMR tube, a white precipitate was immediately produced. The ¹¹B NMR spectrum (80 MHz) of the reaction solution showed one peak at δ 27.2, which was assigned to the 9-BBN dimer (the same chemical shift was obtained when the 9-BBN dimer is dissolved in CD₂-Cl₂). A resonance corresponding to **2** was absent. The ¹H NMR spectrum (250 MHz) of the reaction solution further confirmed that the 9-BBN dimer had been produced.

Reaction of **2 with B(C₆F₅)₃. Formation of [Yb(THF)₆][HB(C₆F₅)₃]₂, **3**.** A 50 mL flask was charged with 177 mg (0.250 mmol) of **2** and 256 mg (0.500 mmol) of B(C₆F₅)₃. Approximately 20 mL of THF was condensed into the flask at -78 °C. The flask was warmed to room temperature and stirred for 1 h. Initially, the ¹¹B NMR spectrum (80 MHz) of the reaction solution indicated the presence of the [HB(C₆F₅)₃]⁻ anion (δ -24.2 (d, ¹J_{BH} = 90 Hz)) and the 9-BBN dimer (δ 28.7). After some time, the 9-BBN dimer changed to an organoborane (δ 57.6 (br s)). The solvent was removed and the yellow residue was washed with 3 × 5 mL of hexane. Crystals of **3** were grown from a saturated Et₂O solution at -40 °C. The single-crystal X-ray diffraction structure and ¹H NMR spectrum of **3** indicated that Et₂O and THF were coordinated to the Yb cation. Some solvent ligands were removed by vacuum-drying solid **3**. As determined by elemental analysis, one Et₂O and two THF ligands remained in the molecule ([Yb(OEt₂)(THF)₂][HB(C₆F₅)₃]₂). Anal. Calcd for C₄₈H₂₈O₃F₃₀YbB₂ (one Et₂O and two THF remain): C, 40.67; H, 1.99%. Found: C, 40.18; H, 1.94%. A yield of 189 mg of [Yb(OEt₂)(THF)₂][HB(C₆F₅)₃]₂ (53% based on B(C₆F₅)₃) was obtained. Solid-state IR (KBr): 2983 (s), 2912 (s), 2842 (m), 2375 (m), 2317 (m), 1645 (s), 1603 (w), 1553 (sh), 1513 (vs), 1468 (vs), 1401 (m), 1373 (m), 1331 (w), 1316 (w), 1274 (s), 1172 (w), 1109 (vs), 968 (vs), 913 (m), 892 (m), 860 (m), 787 (w), 757 (m), 728 (w), 686 (w), 663 (m), 602 (m), 567 (m) cm⁻¹. ¹¹B NMR (80 MHz, THF): δ -24.5 (d, ¹J_{BH} = 90 Hz). ¹H NMR (250 MHz, *d*₈-THF): δ 3.14 (q, CH₂ of Et₂O, ³J_{HH} = 7 Hz), 0.87 (t, CH₃ of Et₂O, ³J_{HH} = 7 Hz). ¹H{¹¹B} NMR (250 MHz, *d*₈-THF): δ 3.91 (s, HB).

Acknowledgment. This work was supported by the National Science Foundation through Grants CHE 99-01115 and CHE 02-13491.

Supporting Information Available: Three crystallographic files in CIF format and figures showing molecular structures of **2** and **3** and relevant ¹H NMR, ¹¹B NMR, and IR spectra. This material is available free of charge via the Internet at <http://pubs.acs.org>.

IC030249S